Discover Oncology

ANALYSIS Open Access

Elevated CD14 in B cells associates with reduced ovarian cancer risk via CD80 + dendritic cell interaction: a multi-omics study

Mengyu Zheng[1*]

*Correspondence:
Mengyu Zheng
zhengmengyu666@163.com
[1]Department of Obstetrics and gynecology, Affiliated People's Hospital of NingBo University, 251 Baizhang east Road, Ningbo 315040, Zhejiang, People's Republic of China

Abstract

Introduction Ovarian cancer (OC) is a highly aggressive malignancy characterized by a complex immune microenvironment. B cells, essential components of immunological regulation, have been implicated in the progression of ovarian cancer. However, the precise mechanisms by which B cells and immune molecules influence ovarian cancer risk remain poorly understood.

Methods This study employed single-cell RNA sequencing (scRNA-seq) to analyze peripheral blood mononuclear cells (PBMCs) from ovarian cancer patients and healthy donors. Differential gene expression analysis identified CD14 as a critical gene in B cells. Mendelian randomization (MR) analysis, using exposure data from eQTL and pQTL databases, was performed to evaluate the association between CD14 and ovarian cancer risk. Mediation analysis was conducted to assess the role of CD80 on myeloid dendritic cells in mediating the relationship between CD14 and ovarian cancer.

Results The analysis demonstrated that CD14 expression was significantly downregulated in B cells from ovarian cancer patients compared to healthy donors. MR analysis revealed a significant association between elevated CD14 expression and reduced ovarian cancer risk. Mediation analysis indicated that CD80 mediated 26.2% of this effect.

Conclusion These findings highlight CD14 as a key regulator of ovarian cancer risk, with CD80 serving as a mediator of the immune response in this context. This study provides insights into potential immune modulation strategies for ovarian cancer therapy.

Keywords CD14, CD80, Ovarian Cancer, Mendelian Randomization, Immune Cells

1 Introduction

Ovarian cancer (OC) is the most prevalent malignant gynecological neoplasm, with high-grade serous ovarian cancer (HGSOC) accounting for approximately 75% of all cases [1]. The 5-year survival rate of OC remains alarmingly low at around 30% [2], primarily due to late-stage diagnoses (stage III or IV). In 2020, the United States reported

21,750 newly diagnosed OC cases, of which 13,940 resulted in death [3]. Factors contributing to the poor prognosis of OC include delayed diagnosis, chemotherapy resistance, high recurrence rates, and both local and distant metastases. These challenges underscore the need for extensive research into more effective treatments.

In recent years, the tumor microenvironment (TME) of OC has garnered significant attention. The TME consists of cellular components such as immune cells, tumor cells, and stromal cells, as well as noncellular elements, including cytokines, growth factors, and metabolites [4]. Immune cells play a pivotal role in OC progression. Advances in immunology have demonstrated that B cells have a dual function within the immune milieu of ovarian cancer [5]. On one hand, B cells contribute to immune surveillance by producing specific antibodies against tumor cells and by serving as antigen-presenting cells that activate T cells to elicit tumor-specific immune responses [6]. On the other hand, B cells can promote tumor immune evasion and facilitate tumor growth and metastasis through the secretion of immunosuppressive cytokines, such as IL-10, or through interactions with T cells [7]. Despite these critical roles, research on B cells in ovarian cancer remains limited, necessitating further investigation.

Single-cell RNA sequencing (scRNA-seq) is a powerful technique for examining cellular heterogeneity, enabling the identification of genomic alterations and distinct transcriptomic states at single-cell resolution [8]. This technology allows for the precise classification of tumor-associated immune cell populations and the characterization of the heterogeneity within the tumor microenvironment. scRNA-seq has proven invaluable in oncology, facilitating the discovery of novel tumor biomarkers and advancing personalized immunotherapy approaches for improved cancer treatment outcomes [9].

Mendelian randomization (MR) is a theoretical approach that utilizes genetic variation as an instrumental variable (IV) to assess potential causal relationships between exposures and outcomes [10]. By leveraging the random allocation of genetic variants during meiosis, MR reduces the influence of confounding factors and reverse causation, thus mimicking the effects of randomized controlled trials [11]. MR analysis employs expression quantitative trait loci (eQTL) and protein quantitative trait loci (pQTL), which are single-nucleotide polymorphisms (SNPs) associated with gene expression, as instrumental variables to investigate genes that may serve as therapeutic targets. This approach has been widely applied to the study of various diseases [12, 13].

In this study, we used single-cell RNA sequencing to analyze differential gene expression in B cells within the context of ovarian cancer. By integrating eQTL and pQTL data with Mendelian randomization, we identified key genes and assessed the role of immune cells in ovarian cancer risk through mediation analysis. This comprehensive approach provides new insights into the molecular mechanisms linking immune cells to ovarian cancer and offers potential clinical implications (Fig. 1).

2 Methods

2.1 Single-cell RNA sequencing and differential expression genes analysis

Single-cell RNA sequencing (scRNA-seq) data from the peripheral blood mononuclear cells (PBMCs) of 6 patients with high-grade serous ovarian cancer (HGSOC) and 6 healthy donors were obtained from the GEO database (GSE264489) [14]. It is important to note that this study exclusively utilized PBMC samples from the GSE264489 dataset; tumor-infiltrating cells or tumor microenvironment samples were not analyzed. HGSOC

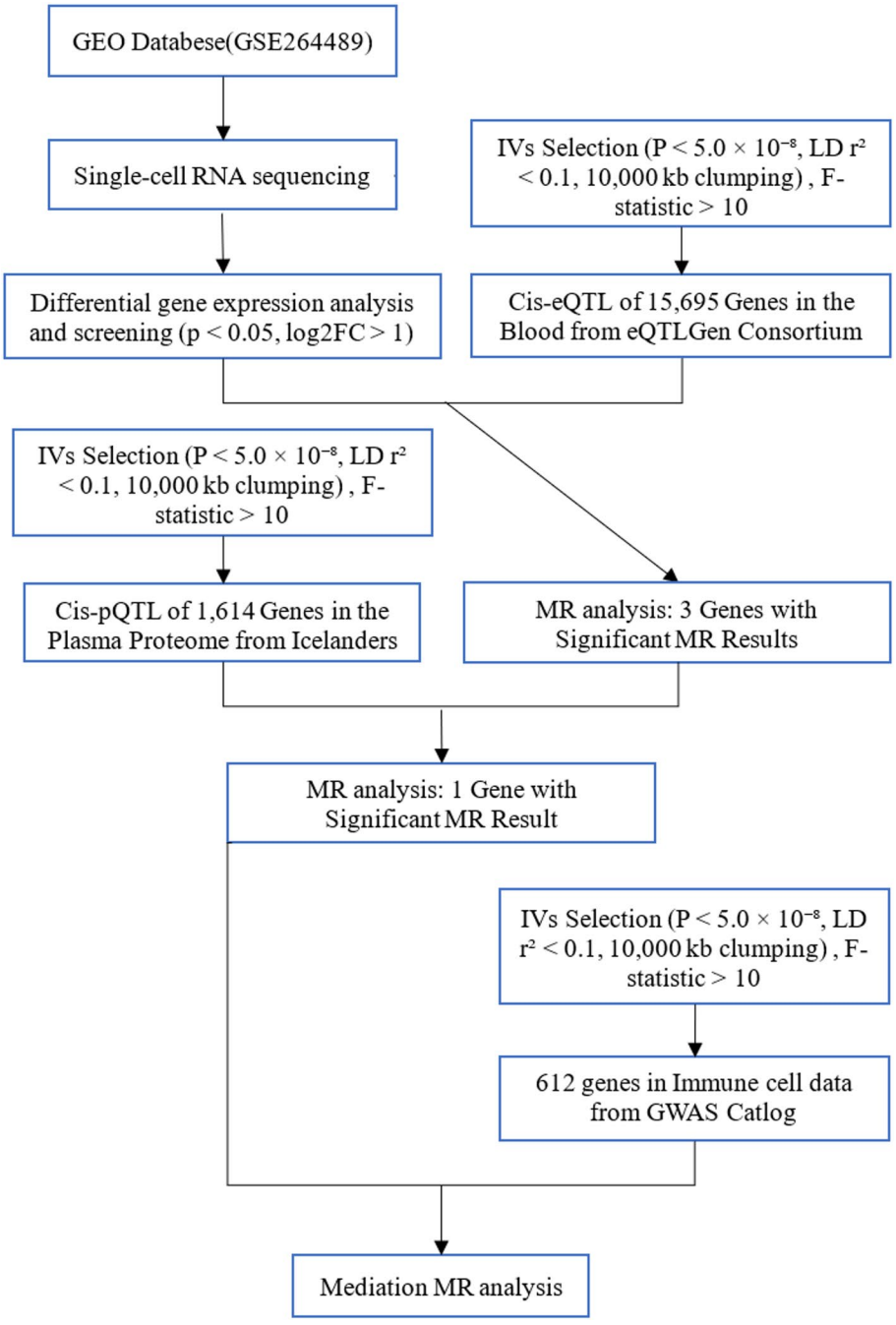

Fig. 1 Study flow chart

patients were divided into two cohorts: 6 patients received platinum-based neoadjuvant chemotherapy (NACT; carboplatin + paclitaxel) prior to surgery. All patients subsequently received adjuant platinum/taxane therapy post-surgery. PBMCs were isolated from whole blood using Lymphosep density gradient centrifugation (600 g, 30 min) [2], washed with DPBS, counted via CytoFLEX flow cytometry, and cryopreserved in X-VIVO™ medium with 10% DMSO at -80°C for ≤ 6 months. Libraries were constructed on the Chromium X platform (10x Genomics Next GEM 3' v3.1) and sequenced on Illumina NextSeq 2000. Seurat objects were generated for each sample, and low-quality

cells were excluded based on the criteria of nFeature_RNA > 50 and percent.mt < 5%. Potential doublets were removed using DoubletFinder (v2.0.3) with an expected doublet rate of 10%(Supplementary Figure S4). The data were subsequently standardized using the LogNormalize method, and the 1,500 most variable genes were selected for further analysis. To account for technical batch effects between samples, we applied Seurat's canonical data integration pipeline. First, integration anchors were identified across individual datasets using the FindIntegrationAnchors function, with parameters set to project principal components 1–30 (dims = 1:30) and stabilize anchor selection via k.filter = 200 to accommodate inter-sample variability. Next, the IntegrateData function was used to merge datasets based on these anchors, generating a batch-corrected expression matrix. Integration efficacy was validated by comparing the distribution of mitochondrial gene content (percent.mt), total RNA counts (nCount_RNA), and detected features (nFeature_RNA) across batches using the VlnPlot function, confirming minimal residual technical variation after integration(Supplementary Figure S1). Principal component analysis (PCA) was conducted, retaining the first 30 principal components. Non-linear dimensionality reduction was performed using t-SNE to visualize cell populations. Cell types were annotated using the SingleR algorithm with the HumanPrimaryCellAtlasData reference. The marker genes of each cell type were annotated using bubble map(Supplementary Figure S2). Differential gene expression analysis was conducted between the ovarian cancer and healthy donor groups. Specifically, for the B cell population, differentially expressed genes were identified, with significance defined as FDR < 0.05 and log2FC > 1(Supplementary Figure S3).

2.2 Differential gene function enrichment analysis

Gene Ontology (GO) enrichment analysis and Kyoto Encyclopedia of Genes and Genomes (KEGG) pathway analysis were performed to determine the biological functions of the chosen significantly differentially expressed genes (monocyte markers). GO enrichment analysis was conducted using the clusterProfiler package, classifying genes into three primary ontologies: Biological Process (BP), Molecular Function (MF), and Cellular Component (CC). Only terms with a p-value < 0.05 were considered significant. Similarly, KEGG pathway analysis was performed to identify biological pathways associated with these genes, applying the same significance threshold (p-value < 0.05). The results of both GO and KEGG analyses were visualized using bar plots and dot plots, highlighting the most enriched terms or pathways.

2.3 Mendelian randomization analysis of differential genes using eQTL and pQTL data

We performed Mendelian randomization (MR) analysis using expression quantitative trait loci (eQTL) and protein quantitative trait loci (pQTL) data to examine causal relationships between gene expression and disease outcomes. For eQTL analysis, differentially expressed genes from the scRNA-seq data were combined with the eQTLGen database [15]. Single nucleotide polymorphisms (SNPs) were filtered based on p-values < 5.0×10^{-8} and clumped using 1,000 Genomes Project (European population) data with an r^2 < 0.1 threshold and a 10,000 kb clumping window [16]. The eQTL analysis was performed using the eQTLGen database, which includes expression data for 15,695 genes across a large cohort. The FinnGen database, comprising 1,025 cases and 167,189 controls for ovarian cancer, was used for MR analysis. We employed the Inverse Variance

Weighted (IVW) method as the primary analysis, with additional methods including MR-Egger and weighted median to assess the robustness of our findings. To validate the identified genes, we performed pQTL analysis using Icelandic pQTL data [17], applying the same filtering criteria (p-value $< 5.0 \times 10^{-8}$, $r^2 < 0.1$, and 10,000 kb window). This analysis identified 1,614 genes with significant pQTL associations, which were then merged with the positive eQTL results. MR analysis was repeated using the FinnGen ovarian cancer outcome data.

MR analysis was performed using the TwoSampleMR R package, with the Inverse Variance Weighted (IVW) method [18] as the primary approach. Additional MR methods, including MR-Egger, weighted median [19], and mode-based techniques [20], were used to verify robustness. Causal effect estimates were derived using the IVW method, with significance defined as p-values < 0.05 [21]. Sensitivity analyses for heterogeneity and pleiotropy [22] were conducted, and results were presented as effect sizes (β), standard errors, p-values, odds ratios (OR), and 95% confidence intervals (CI). Visualizations included forest plots, scatter plots, and sensitivity analysis plots. The MR-PRESSO test [23] was applied to detect and correct for pleiotropic outliers. The F statistic was calculated to assess the strength of the instrumental variable, defined as: $F = [(N - K - 1)/K] / [R^2 / (1 - R^2)]$, where K is the number of genetic variations and N is the sample size. Weak instrumental variables were deemed unlikely to influence MR outcomes if the F statistic exceeded 10 [24].

2.4 Mediation effect analysis

A two-step mediation analysis was conducted to examine the potential mediating role of immune cells in the association between CD14 expression and OC development. This analysis aimed to determine whether immune cells mediate the effects of CD14 on OC progression. Data on immune cells were obtained from the GWAS catalog (datasets GCST90001391 to GCST90002121), comprising 731 data points related to various immune cells [25]. These data were filtered using the same criteria applied in the eQTL and pQTL analyses (p-value $< 5.0 \times 10^{-8}$, $r^2 < 0.1$, and a 10,000 kb clumping window), resulting in the selection of 612 immune cell IDs for further analysis. A two-step mediated MR analysis was conducted to evaluate the potential mediation effect of immune cells in the relationship between CD14 and OC, as well as the extent of this mediation [26] (Fig. 2). The total effect of CD14 on OC was partitioned into (i) direct effects of CD14 on OC and (ii) indirect effects mediated by CD14 via immune cells. The fraction mediated by immune cells was calculated by dividing the indirect effect by the total effect. This analysis enabled a comprehensive assessment of both direct and mediated influences of CD14 on OC.

3 Results

3.1 Single-cell RNA sequencing-based identification of differential gene expression in B cells

Differential gene expression analyses comparing OC (HGSOC) and healthy donor groups identified 62 differentially expressed genes (DEGs) in B cells with a FDR < 0.05 and log2 fold change (log2FC) > 1. Clustering analysis revealed nine distinct cell populations: monocytes, T cells, NK cells, B cells, HSC-G-CSF, pre-B cells (CD34–), platelets, MEPs (megakaryocyte-erythroid progenitors), and an undefined category (NA) (Fig. 3). Of these, CD14 was identified as a DEG in B cells, showing significant downregulation

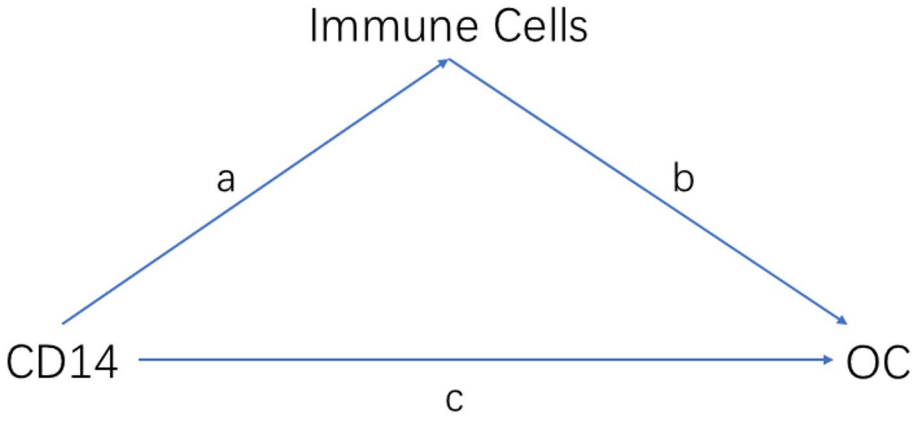

Fig. 2 A graph depicting the methodologies employed in this study. The overall impacts of CD14 and OC were analyzed as follows: (1) indirect effects, utilizing a two-step approach (where **a** represents the influence of CD14 on immune cells, **b** denotes the effect of immune cells on OC, and **c** signifies the total effect of CD14 as the exposure and OC as the outcome; the indirect effect is calculated as ($c' = c - a \times b$))

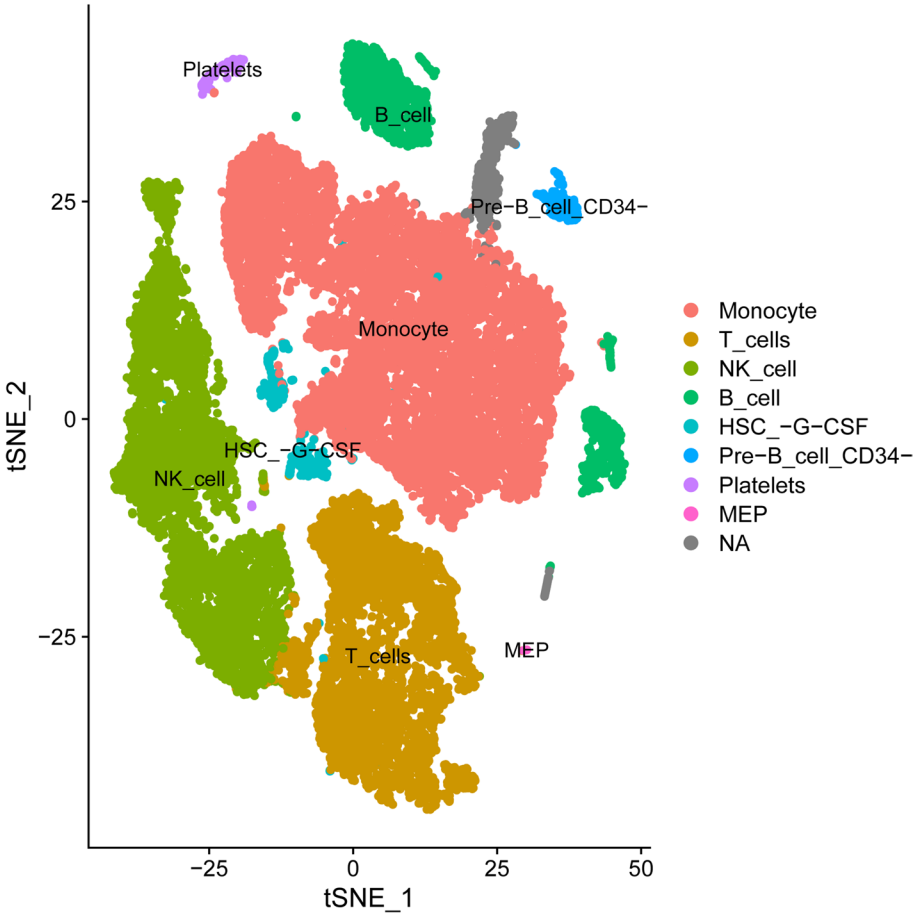

Fig. 3 t-SNE analysis revealing distinct clustering between cells from ovarian cancer patients and healthy donors. Nine major cell populations were identified, including Monocytes, T cells, NK cells, B cells, HSC-G-CSF, Pre-B cells (CD34–), Platelets, MEPs (megakaryocyte-erythroid progenitors), and an undefined category (NA)

in HGSOC patients compared to healthy donors (Fig. 4). In contrast to B cells, CD14 expression in monocytes did not show significant differential expression between ovarian cancer patients and healthy controls in our dataset (adjusted $p > 0.05$).

3.2 GO and KEGG pathway analyses

GO analyses revealed significant enrichment for the following Molecular Function (MF) terms: phosphatidic acid binding, protein serine/threonine kinase inhibitor activity, protein kinase inhibitor activity, and kinase inhibitor activity, with the criterial of adjusted P-values < 0.05. KEGG pathway analyses demonstrated significant enrichment in the glycosylphosphatidylinositol(GPI)-anchor biosynthesis, mTOR signaling, and autophagy-animal pathways, with the criterial of adjusted P-values < 0.05 (Fig. 5).

3.3 Mendelian randomization analysis

The findings of the MR analysis are summarized in Table 1. Using the Inverse Variance Weighted (IVW) method, we identified a significant association between increased CD14 (eQTL) expression and reduced ovarian cancer risk ($P = 0.042$, OR = 0.854, 95% CI = 0.734–0.995). The MR-Egger method also revealed a significant inverse association between elevated CD14 levels and ovarian cancer risk ($P = 0.045$, OR = 0.737, 95% CI = 0.555–0.977). Additionally, the IVW method indicated a significant inverse

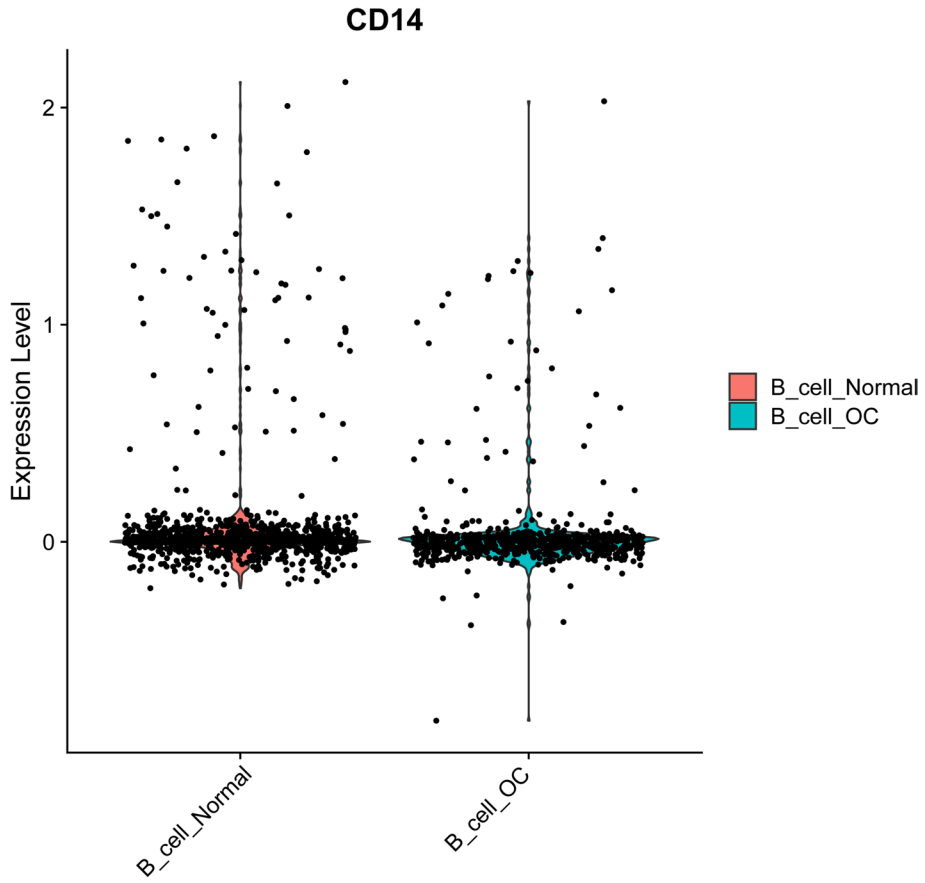

Fig. 4 A bar chart showing that CD14 expression in the B cells of ovarian cancer patients was significantly decreased ($p < 0.05$)

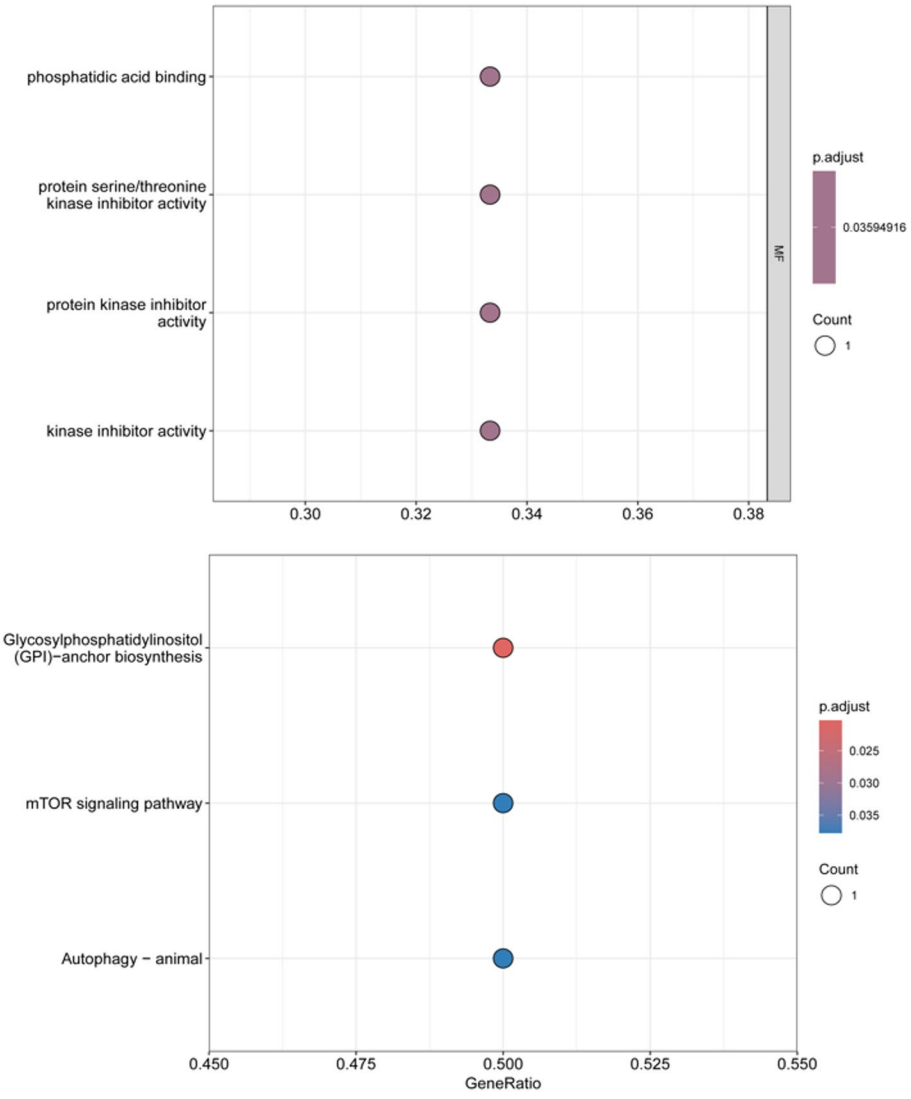

Fig. 5 A bar chart of GO and KEGG analysis results. *P*<0.05

correlation between higher CD14 (pQTL) levels and ovarian cancer incidence ($P = 0.035$, OR = 0.793, 95% CI = 0.639–0.984).

Cochran's Q test was used to assess heterogeneity, while the MR-Egger intercept was applied to evaluate horizontal pleiotropy. As shown in Table 2, no heterogeneity was detected, with all p-values > 0.05. Funnel plots were generated for each MR analysis to illustrate study heterogeneity (Figs. 6 and 7; Table 2). The MR-Egger intercept test revealed no evidence of horizontal pleiotropy ($P > 0.05$), and the MR-PRESSO global test did not identify any outliers (Figs. 6 and 7; Table 2). Multiple sensitivity analyses confirmed the robustness of these MR findings (Figs. 6 and 7). A forest plot displaying the causal effects of each SNP on ovarian cancer risk and the instrumental variables used in the analysis is presented in Figs. 6 and 7.

3.3.1 The relationship between CD14 and immune cells

The association between CD14 expression and immune cells was examined using GWAS data, which revealed a strong correlation between CD14 and two immune cell categories

Table 1 The results of MR analysis

Exposure	Outcome	MR methods	SNPs	*P*-Value	OR(95%CI)	F
CD14(eQTL)	Ovarian Cancer	MR Egger	25	0.045	0.737 (0.555–0.977)	171.660
		Weighted median	25	0.050	0.817 (0.668-1.000)	
		Inverse variance weighted	25	0.042	0.854 (0.734–0.995)	
		Simple mode	25	0.151	0.790 (0.580–1.078)	
		Weighted mode	25	0.064	0.806 (0.649–1.002)	
CD14(pQTL)	Ovarian Cancer	MR Egger	32	0.088	0.661 (0.418–1.047)	91.729
		Weighted median	32	0.139	0.793 (0.583–1.078)	
		Inverse variance weighted	32	0.035	0.793 (0.639–0.984)	
		Simple mode	32	0.748	0.911 (0.520–1.599)	
		Weighted mode	32	0.243	0.827 (0.604–1.131)	
CD80	Ovarian Cancer	MR Egger	25	0.062	0.811 (0.659-1.000)	169.140
		Weighted median	25	0.013	0.811 (0.687–0.957)	
		Inverse variance weighted	25	0.005	0.852 (0.762–0.952)	
		Simple mode	25	0.207	0.861 (0.686–1.080)	
		Weighted mode	25	0.058	0.848 (0.721–0.997)	
CD14	CD80	MR Egger	5	0.572	1.198 (0.684–2.098)	72.078
		Weighted median	5	0.024	1.340 (1.039–1.729)	
		Inverse variance weighted	5	0.021	1.294 (1.040–1.609)	
		Simple mode	5	0.139	1.390 (0.980–1.971)	
		Weighted mode	5	0.157	1.386 (0.959–2.004)	

Table 2 The results of heterogeneity testing and Pleiotropy testing

Exposure	Outcome	Heterogeneity				Pleiotropy	
		MR Egger		IVW		MR Egger	
		Q	*P*	Q	*P*	Intercept	*P*
CD14(eQTL)	Ovarian Cancer	10.501	0.988	11.983	0.980	0.034	0.236
CD14(pQTL)	Ovarian Cancer	33.500	0.301	34.362	0.310	0.025	0.387
CD80	Ovarian Cancer	16.210	0.846	16.501	0.869	0.010	0.595
CD14	CD80	0.638	0.888	0.723	0.948	0.022	0.790

($P<0.05$). CD80 on myeloid dendritic cells (DCs) exhibited the strongest association with CD14, and five highly correlated independent SNPs were selected for causal analysis. As shown in Table 1, the IVW method identified a significant association between elevated CD14 levels and increased CD80 expression on myeloid DCs ($P=0.021$, OR = 1.294, 95% CI = 1.040–1.609). Similarly, the Weighted Median method showed a significant association between higher CD14 levels and increased CD80 levels on myeloid DCs ($P=0.024$, OR = 1.340, 95% CI = 1.039–1.729). Visualizations of the MR analysis are provided in Fig. 8. Table 2 demonstrates the absence of pleiotropy and heterogeneity.

3.3.2 Relationships between immune cells and ovarian cancer

GWAS data from immune cells indicated that CD80 expression on myeloid DCs was associated with OC risk. Twenty-five SNPs with significant correlations were selected for causal analysis. Table 1 shows that the IVW method identified a significant association between increased CD80 levels on myeloid DCs and reduced OC risk ($P=0.005$, OR = 0.852, 95% CI = 0.762–0.952). The Weighted Median method also revealed that higher CD80 levels on myeloid DCs were significantly linked to a decreased risk of ovarian cancer ($P=0.013$, OR = 0.811, 95% CI = 0.687–0.957). Visualizations of the MR analysis are shown in Fig. 9. Table 2 confirms the absence of pleiotropy and heterogeneity.

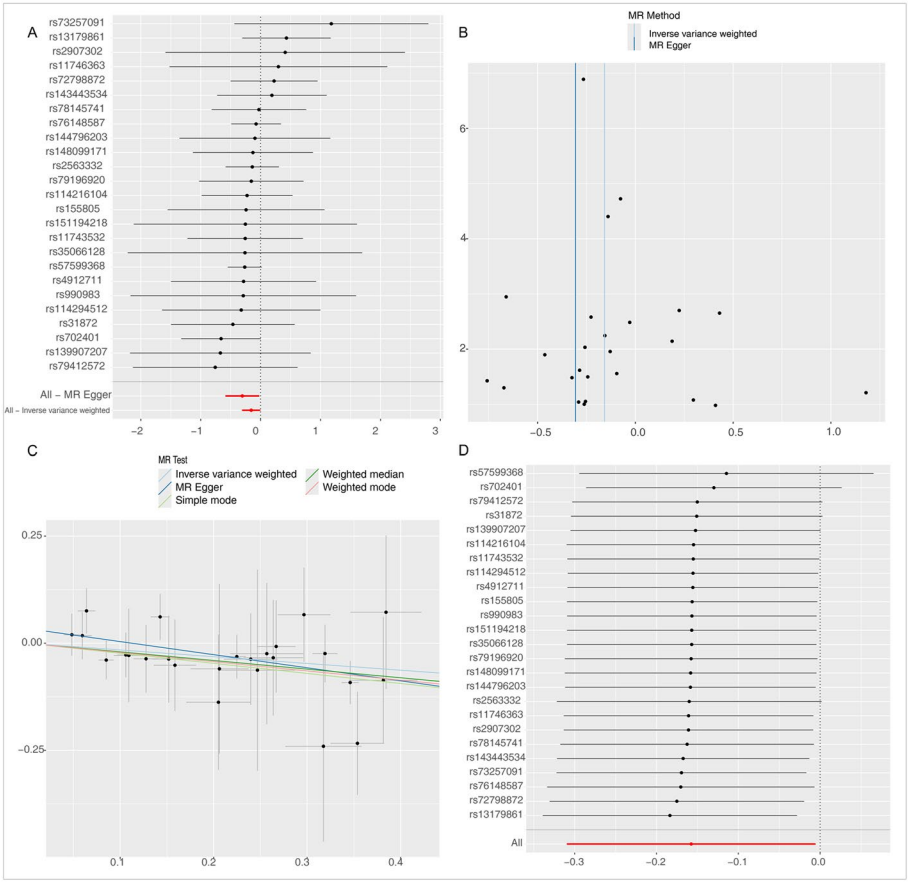

Fig. 6 MR Analysis of CD14 (eQTL) and OC. **A** Leave-one-out forest map; **B** funnel diagram; **C** Scatter plot: Lines in black, red, green, and blue represent IVW, MR-Egger, weighted median, and weighted mode methods; D Forest map for the sensitivity analysis

3.3.3 The mediating role of immune cells in the CD14-ovarian cancer relationship

We observed that increased CD14 expression was associated with a lower incidence of OC. Additionally, elevated CD14 expression was linked to higher CD80 levels on myeloid DCs, which in turn correlated with a reduced risk of ovarian cancer. Mediation analysis estimated that CD80 on myeloid DCs mediated 26.2% of the effect of elevated CD14 levels on reduced OC risk (Fig. 10).

4 Discussion

This study is the first to demonstrate that elevated CD14 expression in B lymphocytes is associated with a reduced risk of OC. Notably, CD14 expression did not significantly differ in monocytes between ovarian cancer patients and healthy controls, suggesting that the transcriptional alteration we observed may be specific to the B cell compartment in this context. Additionally, CD80 on myeloid dendritic cells was found to significantly mediate the relationship between CD14 and OC risk, with an estimated mediation effect of 26.2%. GO and KEGG pathway analyses further identified key biological processes and signaling pathways related to immune regulation, offering novel insights into the immune microenvironment of ovarian cancer. Although CD14 was not the top-ranking DEG, it was among the few differentially expressed genes in B cells that simultaneously met statistical significance, biological relevance, and the availability of strong eQTL and

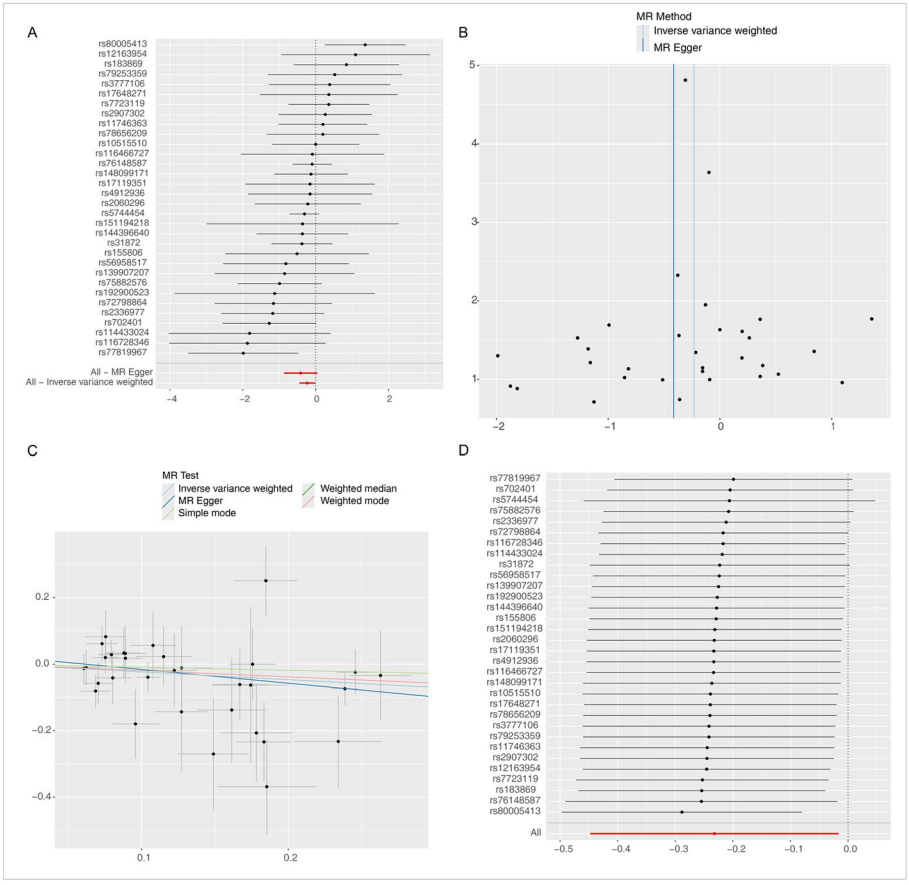

Fig. 7 MR Analysis of CD14(pQTL) and OC. **A** Leave-one-out forest map; **B** funnel diagram; **C** Scatter plot: Lines in black, red, green, and blue represent IVW, MR-Egger, weighted median, and weighted mode methods; **D** Forest map for the sensitivity analysis

pQTL instruments required for Mendelian randomization analysis. This integrative criterion guided its prioritization for downstream causal inference.

The role of B cells in the tumor microenvironment (TME) is two-fold. On the one hand, B cells may promote tumor initiation and progression by producing immunosuppressive cytokines (e.g., IL-10, TGF-β) and interacting with T cells to create an immunosuppressive microenvironment [27, 28]. On the other hand, as antigen-presenting cells (APCs), B cells can interact with T cells to exert anti-tumor immune effects [29]. In the OC immune microenvironment, the role of B cells may be influenced by CD14, an important immune receptor that recognizes pathogen-associated molecular patterns (PAMPs) and modulates immune responses [30, 31]. In this study, we found that increased CD14 expression in B cells was associated with a reduced risk of OC. By interacting with other immune cells in the TME, CD14 may help balance the immune response, preserving effective immune surveillance while preventing tumor proliferation driven by an overactive immune response [6]. Furthermore, the enrichment of phosphatidic acid binding and kinase inhibitor activity in GO analysis supports the critical role of CD14 in immune cell activation and signal transduction. However, we acknowledge that the enrichment analysis was performed on a relatively limited set of QTL-supported DEGs, resulting in a gene count of 1 per term in some cases. As such, the functional interpretations should be considered exploratory and warrant further validation. These

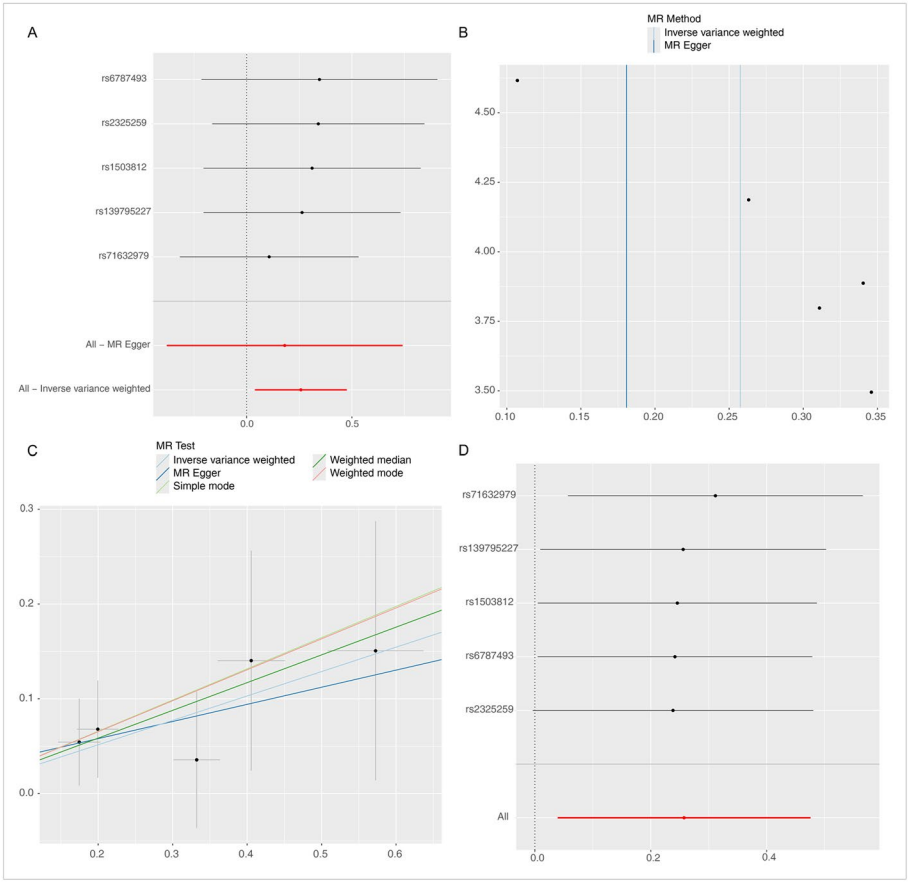

Fig. 8 MR Analysis of CD14 and CD80. **A** Leave-one-out forest map; **B** funnel diagram; **C** Scatter plot: Lines in black, red, green, and blue represent IVW, MR-Egger, weighted median, and weighted mode methods; **D** Forest map for the sensitivity analysis

findings suggest that targeting CD14 could represent a promising strategy for OC immunotherapy, particularly as a means of modulating the immune microenvironment and enhancing immune responses.

CD80 plays a critical role in the immune response of myeloid dendritic cells. As a co-stimulatory molecule, CD80 enhances T cell activation and initiates immune responses by binding to CD28 on T cells [32]. This interaction not only prevents T cell overactivation and activation-induced cell death but also enhances cytokine sAecretion (e.g., IL-2), promotes the proliferation of CD4 + T cells, and augments the cytotoxicity of CD4 + and CD8 + T cells [33]. Through these mechanisms, CD80 enhances the immune response, aiding in the clearance of tumor cells. Additionally, evidence suggests that CD80 competes with PD-L1, a mechanism that may reduce immune escape by tumors. For example, transfecting the CD80 gene into human tumor cells has been shown to suppress PD-L1-mediated immunosuppression and restore T cell activation, further underscoring the role of CD80 in overcoming immune escape [34, 35]. The current study suggests that elevated CD14 expression may mediate the immune microenvironment in OC by increasing CD80 levels. Specifically, increased CD14 may reduce OC risk by enhancing CD80 expression and activating the immune response, potentially limiting tumor cell proliferation and spread. However, these hypotheses require further investigation, as they currently lack sufficient experimental and literature-based validation.

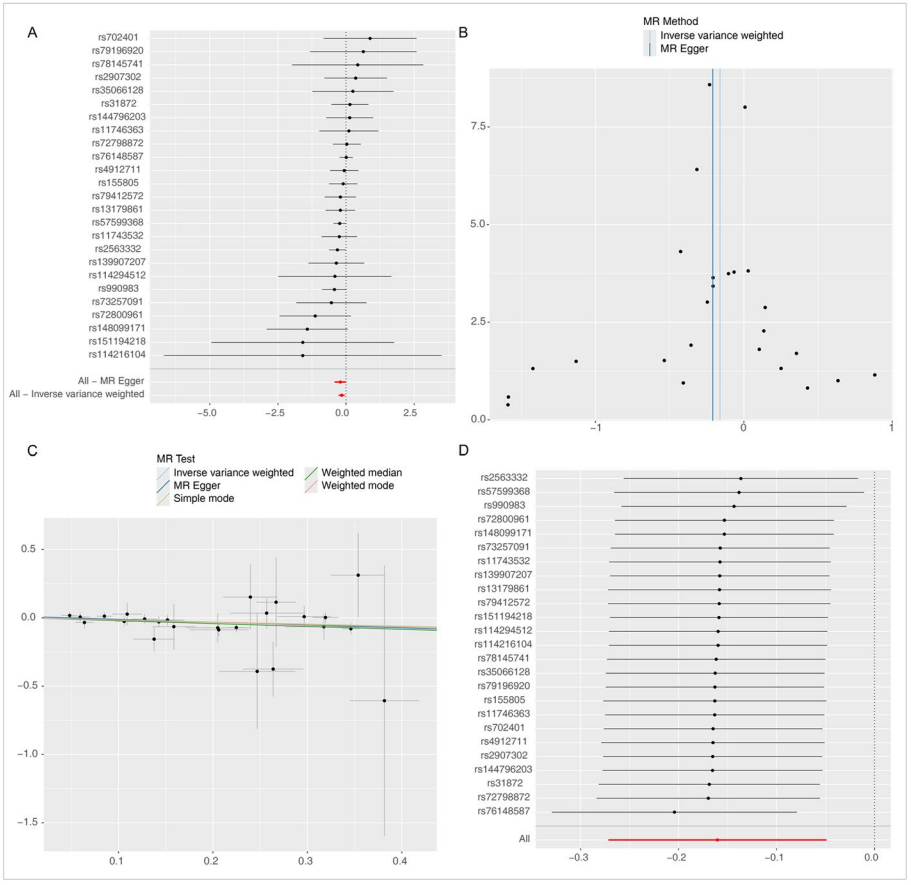

Fig. 9 Results of MR Analysis of CD80 and OC. **A**: Leave-one-out forest map; **B** funnel diagram; **C** Scatter plot: Lines in black, red, green, and blue represent IVW, MR-Egger, weighted median, and weighted mode methods; **D** Forest map for the sensitivity analysis

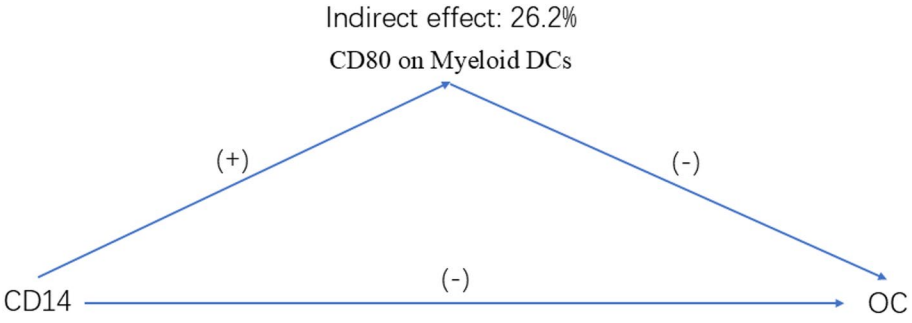

Fig. 10 Schematic overview of the mediating effect of CD80

One of the key strengths of this study is the use of MR analysis combined with eQTL and pQTL data, providing more robust causal inference compared to traditional observational studies. This approach minimizes bias and offers a solid foundation for understanding the immune mechanisms underlying ovarian cancer. The IVW method yielded significant and stable results, with no evidence of heterogeneity or pleiotropy, further supporting the reliability of the findings. Notably, mediation analysis identified CD80 as a mediator between CD14 expression and ovarian cancer risk, highlighting a potential new target for immunotherapy. However, this study has several limitations. First,

while the MR Analysis provided genetic evidence to support the priority of biomarkers for ovarian cancer, the MR Analysis only supported biomarker associations, not functional causation, and the results depended on the quality and range of available eQTL and pQTL data, which may be limited by sample size and population-specific factors that may affect the generality of the results. Second, while single-cell RNA sequencing resolved CD14 expression heterogeneity across B cell subsets, the functional relevance of elevated CD14 in modulating B cell crosstalk with dendritic cells or tumor cells remains mechanistically undefined. While this study highlights the peripheral immune response, we recognize that the modulation of CD14 and CD80 may also influence tumor-infiltrating immune cells. Future studies will focus on the impact of CD14/CD80 modulation within the tumor microenvironment, including how these immune cells respond to changes in immune regulation and their potential role in tumor progression. Third, While this study provides significant insights into the peripheral immune response, we acknowledge that it does not capture tumor-infiltrating lymphocytes or other immune cells within the tumor microenvironment. Future studies incorporating tumor tissue samples will be essential to fully understand the complex interactions between the tumor and immune cells. Moreover, although our transcriptomic data suggest the presence of a $CD14^+$ B cell subset, we were unable to validate this population at the protein level using multicolor flow cytometry or immunohistochemistry due to current limitations in sample accessibility and laboratory resources. Finally, the genetic instruments used in MR analysis may be affected by the complexity of the gene-phenotype relationship. Future studies involving larger and more diverse populations are needed to enhance the robustness and external validity of these results.

5 Conclusion

Our study reveals an observational association between elevated CD14 expression in B cells and a reduced risk of ovarian cancer, with CD80 activity in myeloid dendritic cells statistically accounting for 26.2% of this association based on Mendelian randomization analysis. Nonetheless, the broader immune regulatory mechanisms involving CD14 in OC remain unclear. Further research is necessary to identify additional mediators and validate the functional roles of these molecules within the tumor immune microenvironment.

5.1 Future perspectives

Building upon the prioritization of CD14 through our two-phase translational framework, future studies will focus on refining its cell-type specificity and functional relevance in ovarian cancer. First, we will use single-cell multi-omics to map the transcriptional and epigenetic regulatory network governing CD14 expression in tumor-infiltrating B cells, while systematically identifying B cell–specific DEGs with minimal expression in other immune lineages. Second, CD14's biological impact will be evaluated using B cell-specific CD14 conditional knockout models to test effects on tumor growth and immune infiltration. Third, clinical-translational efforts will aim to validate the presence of $CD14^+$ B cells and their association with $CD80^+$ dendritic cells through multicolor flow cytometry, immunohistochemistry, and spatial transcriptomics in human samples. Together, these steps aim to confirm transcriptomic observations, delineate functional pathways, and establish CD14 as a biologically and clinically meaningful immunoregulatory target in ovarian cancer.

Supplementary Information

The online version contains supplementary material available at https://doi.org/10.1007/s12672-025-02956-8.

Supplementary Material 1—Batch effect correction validation across integrated samples. (A-C) Violin diagram shows the distribution of key cell quality control indicators in all integrated samples after application of the Seurat integration pipeline: (A) number of genes detected per cell (nFeature_RNA), (B) total RNA count per cell (nCount_RNA), and (C) mitochondrial gene content (percent.mt). Each violin represents a different biological sample

Supplementary Material 2—Marker gene expression. The marker gene expression bubble plot of canonical genes that used during cell type annotation process. The red the dot the higher the expression, the larger the dot the larger percent of cell's detected expression that gene

Supplementary Material 3—Volcano map of B-cell specific differentially expressed genes (DEGs). Red dots indicate significantly up-regulated genes, and black dots indicate down-regulated genes. CD14 (highlighted in a red diamond) is marked as a key up-regulated marker (***Log2FC> 1, adjusted p-value < 0.05***)

Supplementary Material 4—Monocyte and B cell marker gene expression. Monocyte and B Cell marker gene CSF1R and CD79A expression between the two cells

Acknowledgements
We would like to thank MogoEdit (https://www.mogoedit.com) for its English editing during the preparation of this manuscript.

Author contributions
Mengyu Zheng spearheaded the study's design, undertook data analysis, and played a key role in manuscript drafting and modifications. Mengyu Zheng also contributed to the foundational conceptualization and layout of the research. Mengyu Zheng has evaluated and given affirmation to the manuscript's final rendition.

Funding
No funding was received for this work from any governmental, private, or non-profit entities.

Data availability
The research-related data have been stored in publicly available repositories.Exposure Data: The eQTL data used in this study are publicly available and can be accessed through the eQTLGen database under the following link: https://www.eqtlgen.org/cis-eqtls.html. The pQTL data in this study are accessible via the deCODE Genetics website at the following link: https://www.decode.com/summarydata/.Immune Cells Data: The immune cells data have been deposited in the GWAS catalog under accession codes Database ID 'GCST90001391 to GCST90002121', comprising a total of 731 immune cells. The data can be accessed at: https://www.ebi.ac.uk/gwas/home.Outcome Data: The outcome data were obtained from the FinnGen database and can be accessed at the following link: https://storage.googleapis.com/finngen-public-data-r9/summary_stats/finngen_R9_C3_OVARY_EXALLC.gz.

Declarations

Ethics approval and consent to participate
For this investigation, summary statistics from publicly available published studies and consortia were utilized. Consent was given by participants in the original research, and ethical approval was granted by relevant review boards. Given that this study did not involve individual data usage, no extra ethical approval was required.

Consent for publication
Not applicable.

Competing interests
The authors declare no competing interests.

Received: 26 December 2024 / Accepted: 10 June 2025
Published online: 15 June 2025

References

1. da Costa AABA, Baiocchi G. Genomic profiling of platinum-resistant ovarian cancer: the road into druggable targets. Semin Cancer Biol. 2021;77:29–41.
2. Lheureux S, Braunstein M, Oza AM. Epithelial ovarian cancer: evolution of management in the era of precision medicine. CA Cancer J Clin. 2019;69:280–304.
3. Siegel RL, Miller KD, Jemal A. Cancer statistics, 2020. CA Cancer J Clin. 2020;70:7–30.
4. Xiong J, Fu Y, Huang J, Wang Y, Jin X, Wan X, et al. Metabolic and senescence characteristics associated with the immune microenvironment in ovarian cancer. Front Endocrinol (Lausanne). 2023;14:1265525.
5. Downs-Canner SM, Meier J, Vincent BG, Serody JS. B cell function in the tumor microenvironment. Annu Rev Immunol. 2022;40:169–93.
6. Hu Q. Atlas of breast cancer infiltrated B-lymphocytes revealed by paired single-cell RNA-sequencing and antigen receptor profiling.
7. Xue H, Lin F, Tan H, Zhu Z-Q, Zhang Z-Y, Zhao L. Overrepresentation of IL-10-Expressing B cells suppresses cytotoxic CD4 + T cell activity in HBV-Induced hepatocellular carcinoma. PLoS ONE. 2016;11:e0154815.

8. Balan D, Kampan NC, Plebanski M, Abd Aziz NH. Unlocking ovarian cancer heterogeneity: advancing immunotherapy through single-cell transcriptomics. Front Oncol. 2024;14:1388663.
9. Guruprasad P, Lee YG, Kim KH, Ruella M. The current landscape of single-cell transcriptomics for cancer immunotherapy. J Exp Med. 2021;218:e20201574.
10. Swanson SA, Tiemeier H, Ikram MA, Hernán MA. Nature as a trialist?? Deconstructing the analogy between Mendelian randomization and randomized trials. Epidemiology. 2017;28:653–9.
11. Skrivankova VW, Richmond RC, Woolf BAR, Yarmolinsky J, Davies NM, Swanson SA, et al. Strengthening the reporting of observational studies in epidemiology using Mendelian randomization: the STROBE-MR statement. JAMA. 2021;326:1614–21.
12. Storm CS, Kia DA, Almramhi MM, Bandres-Ciga S, Finan C et al. International Parkinson's Disease Genomics Consortium (IPDGC),. Finding genetically-supported drug targets for Parkinson's disease using Mendelian randomization of the druggable genome. Nat Commun. 2021;12:7342.
13. Genetic insights into therapeutic targets for aortic aneurysms. A Mendelian randomization study - PubMed [Internet]. [cited 2024 Aug 22]. Available from: https://pubmed.ncbi.nlm.nih.gov/35952493/
14. Platinum-based chemotherapy. promotes antigen presenting potential in monocytes of patients with high-grade serous ovarian carcinoma - PubMed [Internet]. [cited 2024 Dec 24]. Available from: https://pubmed.ncbi.nlm.nih.gov/39315092/
15. Finan C, Gaulton A, Kruger FA, Lumbers RT, Shah T, Engmann J, et al. The druggable genome and support for target identification and validation in drug development. Sci Transl Med. 2017;9:eaag1166.
16. Gkatzionis A, Burgess S, Newcombe PJ. Statistical methods for cis-Mendelian randomization with two-sample summary-level data. Genet Epidemiol. 2023;47:3–25.
17. Ferkingstad E, Sulem P, Atlason BA, Sveinbjornsson G, Magnusson MI, Styrmisdottir EL, et al. Large-scale integration of the plasma proteome with genetics and disease. Nat Genet. 2021;53:1712–21.
18. Burgess S, Small DS, Thompson SG. A review of instrumental variable estimators for Mendelian randomization. Stat Methods Med Res. 2017;26:2333–55.
19. Bowden J, Davey Smith G, Haycock PC, Burgess S. Consistent Estimation in Mendelian randomization with some invalid instruments using a weighted median estimator. Genet Epidemiol. 2016;40:304–14.
20. Hartwig FP, Davey Smith G, Bowden J. Robust inference in summary data Mendelian randomization via the zero modal Pleiotropy assumption. Int J Epidemiol. 2017;46:1985–98.
21. Burgess S, Bowden J, Fall T, Ingelsson E, Thompson SG. Sensitivity analyses for robust causal inference from Mendelian randomization analyses with multiple genetic variants. Epidemiology. 2017;28:30–42.
22. Burgess S, Thompson SG. Interpreting findings from Mendelian randomization using the MR-Egger method. Eur J Epidemiol. 2017;32:377–89.
23. Verbanck M, Chen C-Y, Neale B, Do R. Detection of widespread horizontal Pleiotropy in causal relationships inferred from Mendelian randomization between complex traits and diseases. Nat Genet. 2018;50:693–8.
24. Power. and instrument strength requirements for Mendelian randomization studies using multiple genetic variants - PubMed [Internet]. [cited 2024 Aug 22]. Available from: https://pubmed.ncbi.nlm.nih.gov/20813862/
25. Orrù V, Steri M, Sidore C, Marongiu M, Serra V, Olla S, et al. Complex genetic signatures in immune cells underlie autoimmunity and inform therapy. Nat Genet. 2020;52:1036–45.
26. Carter AR, Sanderson E, Hammerton G, Richmond RC, Davey Smith G, Heron J, et al. Mendelian randomisation for mediation analysis: current methods and challenges for implementation. Eur J Epidemiol. 2021;36:465–78.
27. Shen P, Roch T, Lampropoulou V, O'Connor RA, Stervbo U, Hilgenberg E et al. IL-35-producing B cells are critical regulators of immunity during autoimmune and infectious diseases. 2014.
28. Hao S, Chen X, Wang F, Shao Q, Liu J, Zhao H, et al. Breast cancer cell–derived IL-35 promotes tumor progression via induction of IL-35-producing induced regulatory T cells. Carcinogenesis. 2018;39:1488–96.
29. Nielsen JS, Sahota RA, Milne K, Kost SE, Nesslinger NJ, Watson PH, et al. CD20 + tumor-infiltrating lymphocytes have an atypical CD27- memory phenotype and together with CD8 + T cells promote favorable prognosis in ovarian cancer. Clin Cancer Res. 2012;18:3281–92.
30. Sharygin D, Koniaris LG, Wells C, Zimmers TA, Hamidi T. Role of CD14 in human disease. Immunology. 2023;169:260–70.
31. Na K, Oh B-C, Jung Y. Multifaceted role of CD14 in innate immunity and tissue homeostasis. Cytokine Growth Factor Rev. 2023;74:100–7.
32. Duraiswamy J, Turrini R, Minasyan A, Barras D, Crespo I, Grimm AJ et al. Myeloid Antigen-Presenting cell niches sustain antitumor T cells and license PD-1 Blockade via CD28 Costimulation. 2022.
33. Li L, Yang L, Jiang D. Research progress of CD80 in the development of immunotherapy drugs. Front Immunol.
34. Zhang Y, Song Q, Cassady K, Lee M, Tang H, Zheng M, et al. Blockade of trans PD-L1 interaction with CD80 augments antitumor immunity. Proc Natl Acad Sci USA. 2023;120:e2205085120.
35. Zhao Y, Lee CK, Lin C-H, Gassen RB, Xu X, Huang Z, et al. PD-L1:CD80 Cis-Heterodimer triggers the Co-stimulatory receptor CD28 while repressing the inhibitory PD-1 and CTLA-4 pathways. Immunity. 2019;51:1059–e10739.

Publisher's note